Regulatory adenylnucleotide-mediated binding of the PII-like protein SbtB to the cyanobacterial bicarbonate transporter SbtA is controlled by the cellular energy state

Britta Förster[1, a,*], Bratati Mukherjee[1, a], Loraine Rourke[a], Joe A. Kaczmarski[b], Colin J. Jackson[b], G. Dean Price[a,*]

[a] ARC Centre of Excellence in Translational Photosynthesis, Division of Plant Sciences, Research School of Biology, The Australian National University, Canberra, ACT 2601, Australia

[b] Research School of Chemistry, The Australian National University, Canberra, ACT 2601, Australia

[1] both authors contributed equally

* corresponding authors. Email: britta.forster@anu.edu.au or dean.price@anu.edu.au

Keywords: Cyanobacteria, CO_2 concentrating mechanism, PII-like protein SbtB, bicarbonate transporter SbtA, protein-protein interaction, adenylate energy charge response

ABSTRACT

Cyanobacteria have evolved one of the most powerful CO_2 concentrating mechanisms (CCM), supporting high photosynthetic rates with limiting inorganic carbon (Ci), which makes their CCM a desirable system for integration into higher plant chloroplasts to enhance photosynthetic yield. The CCM is driven by active Ci uptake, facilitated by bicarbonate transporters and CO_2 pumps, which locally elevates the CO_2 concentration and carboxylation rate of the primary CO_2 fixing enzyme, Rubisco, inside cytoplasmic micro-compartments (carboxysomes). Ci uptake responds allosterically to Ci supply and light, but the molecular signals and regulators of protein function are unknowns. Functional analyses of sodium-dependent bicarbonate transporters classified as SbtA in *E. coli* support the hypothesis that SbtA activity is negatively regulated through association with its cognate PII-like SbtB protein. Here, we demonstrate that the association of SbtA with SbtB from two phylogenetically distant species, *Cyanobium sp*. PCC7001 and *Synechococcus elongatus* PCC7942, depends on the relative amounts of ATP or cAMP compared to ADP or AMP. Higher ATP over ADP or AMP ratios decreased the formation of SbtA:SbtB complexes, consistent with a sensory response to the cellular adenylate energy charge (AEC=[ATP + 0.5 ADP]/[ATP+ADP+AMP]) and the different binding affinities of these adenylates to SbtB protein trimers. Based on evidence for adenylate ligand-specific conformation changes for the SbtB protein trimer of *Cyanobium sp*. PCC7001, we propose a role for SbtB as a curfew protein locking SbtA into an inactive state as safe-guard against energetically futile and physiologically disadvantageous activation during prolonged low cellular AEC and photosynthetically unfavourable conditions.

INTRODUCTION

Cyanobacteria have evolved one of the most efficient CO_2 concentrating mechanisms (CCM) known to date, which has been fundamental to their adaptability and successful competition in environments providing limited inorganic carbon (Ci) supply for oxygenic photosynthesis and accounts for cyanobacteria contributing 30-80% of the global photosynthetic productivity in the oceans (Liu et al., 1997; Field et al., 1998). This efficiency has fuelled recent efforts of introducing a synthetic, functional cyanobacterial CCM into chloroplasts of staple crop species, predicted to increase photosynthesis and crop yield significantly (Price et al., 2013; McGrath and Long, 2014; Long et al., 2016; Meyer et al., 2016). The cyanobacterial CCM enables active uptake of two Ci species, CO_2 and bicarbonate (HCO_3^-), resulting in the accumulation of large cytoplasmic bicarbonate pools (20-40 mM) (Badger and Andrews, 1982; Price and Badger, 1989) that support carbonic anhydrase (CA)-mediated elevation of the CO_2 concentration around the primary CO_2-fixing enzyme ribulose-1,5-bisphoshate carboxylase/oxygenase (Rubisco). Consequently, Rubisco carboxylation is

53 enhanced over oxygenation, and energetically costly photorespiration suppressed (for review see
54 (Badger and Price, 1992; Kaplan and Reinhold, 1999; Price et al., 2008; Espie and Kimber, 2011;
55 Price, 2011)). To date, five Ci uptake systems have been verified, varying with respect to
56 energization, substrate affinity, flux rates and induction by low Ci conditions (Price, 2011). Two light-
57 dependent, thylakoid-located CO_2 pumps or energy-coupled CAs, Ndh-1_3 and Ndh-1_4 (Maeda et al.,
58 2002; Ohkawa et al., 2002), convert external and internally recaptured CO_2 to HCO_3^-, energized by
59 NADPH and reduced ferredoxin (Ogawa et al., 1985; Maeda et al., 2002; Price et al., 2008). The three
60 types of plasma membrane-located bicarbonate transporters, the ATP-dependent BCT1 complex
61 (Omata et al., 1999) and the HCO_3^-/Na^+ symporters BicA (Price et al., 2004) and SbtA (Shibata et al.,
62 2002), transfer bicarbonate directly from the outside into the cytoplasm upon activation by low Ci
63 conditions and light (Sültemeyer et al., 1998; McGinn et al., 2003). Of particular interest for a
64 synthetic CCM is SbtA due to its ability to function in non-photosynthetic *E. coli* (Du et al., 2014).
65 SbtA requires a Na^+ gradient directed from the outside to the inside of the cell for activity (Shibata et
66 al., 2002; Price et al., 2004). Both CO_2 uptake and HCO_3^- transport are activated by light within
67 seconds (5 and 30 s, respectively) (Badger and Andrews, 1982; Price et al., 2011) and gradually
68 inactivated in the dark, suggesting a link to the state of photosynthetic electron transport or a redox
69 signal (Kaplan et al., 1987), but the molecular mechanisms regulating the activity of specific
70 bicarbonate transporters are largely unknown.
71 An intriguing, highly conserved feature of cyanobacterial genomes is the co-occurrence of
72 the *sbtB* gene, encoding the soluble, PII-like SbtB protein, in the immediate gene neighbourhood of
73 the *sbtA* gene (Rae et al., 2011). Both genes are co-expressed under Ci limitation in *Synechococcus*
74 *elongatus* PCC7942 and *Synechocystis sp.* PCC 6803 (Woodger et al., 2003; Schwarz et al., 2011),
75 suggesting a functional connection between the SbtA and SbtB proteins. This has been underpinned
76 by constitutive inactivation of SbtA-mediated bicarbonate uptake upon co-expression with the
77 cognate SbtB proteins in *E. coli* and by evidence for specific binding of SbtA (SbtA7942) to SbtB
78 (SbtB7942) from *Synechococcus elongatus* PCC7942 (Du et al., 2014). Similarly, a study by Selim *et al.*
79 (Selim et al., 2018) indicated SbtA (SbtA6803) and SbtB (SbtB6803) from *Synechocystis sp.* PCC 6803
80 interacted based on SbtA6803-dependent recruitment of SbtB6803 into membrane fractions under
81 Ci starvation, which was enhanced by addition of ADP or AMP and diminished by cAMP. The authors
82 suggested the cAMP:AMP ratio may indirectly signal the Ci levels in the cell and thus regulate
83 SbtA6803:SbtB6803 complex formation and Ci uptake. However, the HCO_3^- uptake activity of
84 SbtA6803 was not directly measured.
85 SbtB proteins have been classified as non-canonical PII-like members of the multi-functional
86 PII and PII-like protein superfamily consisting of transcriptional and protein activity regulators,

87 environmental signal transducers or sensors, which are widely-distributed across bacteria, archaea
88 and plants. Crystal structures revealed PII and PII-like protein are homotrimers with clefts between
89 monomers forming binding sites for small effector molecules. Typically, effectors are bound in a
90 competitive manner and may bind cooperatively. Common ligands for PII proteins are ATP, ADPs,
91 Mg^{2+} and 2-oxoglutarate (2OG) which impact on protein conformation, particularly the T-loop, and
92 interaction with target proteins (Radchenko et al., 2010; Huergo et al., 2013; Zeth et al., 2014;
93 Forchhammer and Lüddecke, 2016). Ligands identified for cyanobacterial PII-like proteins include
94 ADP and bicarbonate for the carboxysome-associated CPII from *Thiomonas intermedia* (Wheatley et
95 al., 2016), and primarily adenylnucleotides for the SbtB6803 protein (cAMP, AMP, ADP, ATP) (Selim
96 et al., 2018) and SbtB (SbtB7001) protein from *Cyanobium sp.* PCC7001 (cAMP, AMP, ADP, ATP and
97 Ca^{2+}ATP) (Kaczmarski et al., 2019). SbtB6803 and SbtB7001 share the basic architecture, but differ in
98 ligand-coordinating residues, ligand affinities and ligand-induced conformation changes.
99 The energy status of living cells is reflected in the relative abundance of the
100 adenylnucleotides ATP, ADP and AMP and referred to as the cellular adenylate energy charge (AEC),
101 described quantitatively as ([ATP]+0.5[ADP])/([ATP]+[ADP]+[AMP]) (Chapman et al., 1971). The
102 differential binding affinities for ATP, ADP and AMP suggest SbtB may sense the AEC and dynamically
103 interact with SbtA in response to changes in adenylate nucleotide ratios. Here, we investigated (i)
104 the effects of the adenylnucleotides ATP, ADP, AMP and cAMP on the association of SbtA (SbtA7001)
105 from *Cyanobium sp.* PCC7001 and SbtA7942 with their cognate SbtB proteins *in vitro*, based on the
106 hypothesis that the adenylnucleotide ligand-induced structural changes observed for SbtB7001 will
107 determine whether SbtA and SbtB form a complex inactivating SbtA, and (ii) *in vivo* effects of SbtB
108 deletions on SbtA activity in response to Ci availability and light.
109

110 **RESULTS**

111 The impact of small effector molecules on the association of either SbtA7001 or SbtA7942
112 with their cognate SbtB proteins in stable complexes was investigated *in vitro* with membrane-
113 enriched, native protein extracts from the *E.coli* strain DH5α (*E. coli*) and from the bicarbonate
114 transporter deletion strain ΔCS of *Synechococcus elongatus* PCC7942 (*Synechococcus* ΔCS), both co-
115 expressing SbtA7001 and SbtB7001 or SbtA7942 and SbtB7942 from plasmids. The membrane-
116 integral SbtA proteins and the soluble, cytoplasmic SbtB proteins were both present in the
117 membrane-enriched fraction (Fig. S1A), but, contrary to the study by Selim *et al.* (Selim et al., 2018),
118 membrane co-localization was not an unequivocal indicator of SbtA:SbtB complex formation as
119 substantial amounts of either SbtB protein accumulated in the membrane fractions in the absence of
120 SbtA protein (Fig. S1B). Specific binding was therefore evaluated by metal immobilized

121 chromatography (IMAC) purification of SbtA:SbtB complexes with immobilized SbtB as bait and
122 immunological analysis of relative amounts of SbtA and human influenza hemagglutinin (HA)
123 epitope-tagged SbtB proteins with specific antisera. Note that the tagged SbtB7001 and SbtB7942
124 protein monomers are detected at 13 kD consistent with their calculated molecular weights,
125 whereas the apparent molecular weights of SbtA7001 and SbtA7942 monomers are approximately
126 11 kD lower than their calculated molecular weights (23 vs 35 kD and 29 vs 40 kD, respectively) as
127 has been quite commonly observed for membrane proteins and was attributed to altered protein-
128 SDS detergent interactions (Rath et al., 2009).
129
130 **Effects of small charged molecules on SbtA:SbtB complex formation**

131 In the absence of additional effectors, both SbtA-SbtB pairs were dissociated in IMAC
132 binding assays (Fig. 1, S2), which we attributed to the strong dilution effect of extraction and assay
133 buffers on effectors present in intact cells below levels of efficacy. Potential effector molecules
134 reported to interact with PII and PII-like proteins were tested for their ability to facilitate the
135 association of SbtA:SbtB complexes, with particular focus on the adenylnucleotides ATP, ADP, AMP
136 and cAMP and Ca^{2+} that bind to SbtB7001 with micromolar affinities. Since Ca^{2+} enhanced binding of
137 ATP to SbtB7001 *in vitro* (Kaczmarski et al., 2019), and Ca^{2+} and ATP co-occur *in vivo*, we simulated
138 the basal Ca^{2+} levels in cyanobacterial cells (Leganés et al., 2009) including 200 nM $CaCl_2$ as a
139 potential cofactor in binding analyses. On their own, Ca^{2+} and Mg^{2+} (another common cofactor for
140 binding of ATP) did not facilitate SbtA7001:SbtB7001 association (Fig. S2). Individual
141 adenylnucleotides had distinctive effects on the association of both SbtA7001: SbtB7001 and
142 SbtA7942:SbtB7942 protein complexes. SbtA and SbtB remained fully dissociated in the presence of
143 either 2 mM ATP or cAMP, whereas stable SbtA:SbtB complexes formed in the presence of 2 mM
144 ADP or AMP (Fig. 1), showing similar effects on binding interactions for both SbtA-SbtB pairs.
145 Importantly, SbtA-SbtB-effector interactions were qualitatively identical for proteins expressed in *E.*
146 *coli* and *Synechococcus* ΔCS, ruling out confounding effects by potential species-dependent post-
147 translational modifications of either binding partner, adding validity to integrating findings from
148 heterologous expression systems.
149 Amongst small molecule effectors tested, those unable to bind to SbtB7001 were equally
150 ineffective in mediating the binding of either SbtA-SbtB pair. Calvin-Benson-Basham (CBB) cycle
151 intermediates indicative of photosynthetic activity, the substrate ribulose-1,5-bisphosphate (RUBP)
152 and product, 3-phosphoglycerate (3PGA) of the Rubisco reaction, as well as the tricarboxylic acid
153 (TCA) cycle mediate 2OG, a master regulatory metabolite coordinating carbon and nitrogen
154 metabolism (Huergo and Dixon, 2015), did not promote SbtA:SbtB complex formation. A synergistic

155 effect between equimolar 2OG and ATP or ADP, analogous to the prerequisite binding of Mg^{2+}ATP to
156 the *E. coli* PII protein prior to 2OG to become effective, could also be ruled out, as 2OG did not alter
157 the ATP- and ADP-specific effect on the SbtA:SbtB interaction (Fig. 2). HCO_3^- does not bind to the
158 SbtB7001 protein *per se* (Kaczmarski et al., 2019), but considering HCO_3^- is the primary substrate for
159 SbtA, we tested whether bicarbonate levels exerted feedback regulation onto SbtA activity,
160 potentially by varying amounts of inactivate SbtA:SbtB complexes. However, SbtA7001 and
161 SbtB7001 interactions proved to be independent of HCO_3^- across a wide concentration range (0 to
162 100 mM) and irrespective of combinations with 10 mM Mg^{2+}, nano- to millimolar Ca^{2+}
163 concentrations and/or 2 mM ATP or 2 mM AMP (Fig. S2, S3). Interestingly, 10 mM inorganic
164 phosphate (PO_4^{2-}) generally enhanced the formation of SbtA:SbtB complexes (Fig. S4). It is subject to
165 further investigation though, as to whether physiological concentrations of free phosphates affect
166 the interaction of SbtA7001 and SbtB7001 *in vivo*.
167
168 **The adenylnucleotide ratios correlate with the level of SbtA:SbtB association**
169 A link to the adenylate energy charge, suggested by the opposing effects of ATP versus ADP
170 or AMP on SbtA:SbtB complex formation, was explored *in vitro*, simulating different energy charge
171 levels with different molar ratios of ATP:ADP or ATP:AMP within a constant total adenylnucleotide
172 pool of 2 mM (Fig. 3). Irrespective of protein expression in *E. coli* and *Synechococcus* ΔCS, both SbtA-
173 SbtB pairs showed a decrease in amounts of SbtA bound to SbtB with the increasingly higher
174 proportion of ATP over ADP (Fig. 3A-D) and AMP (Fig. S3E, F). Association of SbtA with SbtB and
175 ATP:ADP and ATP:AMP ratios were non-linearly correlated and well fitted by a sigmoidal logistic
176 model with mean adjusted R^2 values of 0.926 ± 0.023 (Fig. S5). Adenylnucleotide ratios supporting
177 50% (AR50), 25% (AR25) or 10% (AR10) of the maximum levels of SbtA bound to SbtB derived from
178 curve fits showed no statistically significant differences between the two SbtA-SbtB pairs and in
179 response to the different adenylnucleotide ratios tested (Table 1, $P > 0.05$)). However, slightly but
180 consistently lower AR values for SbtA74942 indicated lower ATP:ADP and ATP:AMP ratios prevented
181 binding to SbtB than required for the same effect on binding of SbtA7001 and SbtB7001. This may
182 suggest differences in the sensitivity to the intracellular AEC signalled by the molar fraction of ATP in
183 the adenylate pool for the SbtA:SbtB interactions in different cyanobacterial species, but requires
184 more detailed investigation. Similar to ATP, cAMP alone prevented association of both SbtA-SbtB
185 pairs (Fig. 2), and showed increasingly less SbtA was bound to SbtB with higher cAMP:ADP and
186 cAMP:AMP ratios (Fig. 4). Subject to further investigation, the same cAMP levels affected
187 comparatively less SbtA7942 to associate with its cognate SbtB protein than observed for SbtA7001
188 (Table 1). Taken together, when analysed separately, SbtA:SbtB binding appeared to respond to

189 both, molar fractions of ATP and cAMP. One caveat in the experimental design was the application
190 of the same concentration ranges of ATP and cAMP. While ATP concentrations up to 2 mM
191 corresponded closely to the intracellular ATP pools in several bacteria (Thauer et al., 1977; Yaginuma
192 et al., 2014), estimates of cAMP levels in cyanobacterial cells have been up to 1000-fold lower than
193 the intracellular ATP levels (Ohmori and Okamoto, 2004), which suggests the molar fraction of ATP
194 rather than cAMP in the adenylate pool predominantly determines the extent of SbtA:SbtB
195 association *in vivo*.
196
197 **Light-regulated SbtA7942 function *in vivo* is independent of SbtB7942 in *Synechococcus***

198 Regulation of SbtA activity in *E. coli* was closely linked to the presence of the cognate SbtB,
199 where constitutive bicarbonate uptake by SbtA was inactivated when co-expressed with SbtB (Du et
200 al., 2014). In cyanobacteria, however, SbtA and SbtB proteins are both present under low Ci
201 conditions (Fig. 1) and yet SbtA is active to support photosynthesis in the light, which suggests
202 additional levels of regulation tune SbtA function. Potential effects of SbtB on SbtA activity in
203 cyanobacteria were assessed by comparison of photosynthetic performance between *Synechococcus*
204 ΔCS expressing either SbtA7942 and SbtB7942 or SbtA7942 only. Specific SbtA-dependent
205 photosynthetic oxygen evolution and Ci uptake rates were determined by inhibiting both CO_2 pumps
206 with 500 µM ethoxyzolamide (EZ) and performing measurements at pH 8.0 where the prevalent Ci
207 species was HCO_3^-. Direct measurements of radioactively labelled $[^{14}C]HCO_3^-$ uptake by SbtA7942
208 showed bicarbonate uptake rates were unaffected by the presence of up to 1 mM EZ, ruling out
209 inhibitor-induced side effects (Fig. S5). In constant light, SbtA7942-dependent photosynthetic rates
210 were the same in low Ci-induced cell cultures with (SbtAB) or without (SbtA) the SbtB7942 protein
211 expressed (Fig. 5) and indistinguishable with respect to substrate affinities ($k_{0.5}$ 26 ± 5 and 29 ± 4 µM
212 Ci, respectively) and maximum rates of photosynthetic O_2 evolution (V_{max} 179 ± 33 and 164 ± 19
213 µmol mg Chl $^{-1}$ h $^{-1}$, respectively) (Fig. 5, inset). Cell lines co-expressing SbtA and HAHis-tagged SbtB
214 had a 19% lower, but statistically not significant ($P > 0.05$), mean photosynthetic rate (V_{max} 145 ± 14
215 µmol mg Chl $^{-1}$ h $^{-1}$) and HCO_3^- affinity ($k_{0.5}$ 39 ± 15 µM Ci), potentially due to variations in SbtA
216 protein levels. Similarly, steady state HCO_3^- uptake and photosynthetic O_2 evolution rates of SbtA
217 compared to SbtAB showed little differences in response to a change of light intensities from 1400
218 to 200 to 1400 µmol photons m^{-2} s^{-1} in the presence of saturating 250 and 500 µM external Ci (Fig.
219 S7), supporting the notion that SbtB is not involved in modulation of SbtA7942 activity in response to
220 light-dependent changes in photosynthesis that alter Rubisco activity and Ci demand. Since many
221 photosynthetic processes are almost instantaneously inactivated in the dark, bicarbonate uptake by
222 SbtA7942 in light to dark transition and the potential regulatory role of SbtB were assessed by direct

223 uptake measurements of [^{14}C]HCO_3^-. Fully active SbtA7942 was inactivated 15 s after transition from
224 light into darkness, and the initial, fast dark inactivation dynamics of SbtA7942 were unchanged
225 irrespective of the presence of the SbtB7942 protein (Fig. 6). However, this does not rule out a likely
226 role for SbtB in longer dark periods.
227 Reduced growth of the SbtB6803 knockout mutant in *Synechocystis sp.* PCC6803 had been
228 observed under low Ci condition and in low light previously (Selim et al., 2018). Hence,
229 *Synechococcus* ΔCS expressing SbtA7942 and tagged or untagged SbtB7942 or SbtA7942 only were
230 for 10. In contrast to *Synechocystis*, we observed *Synechococcus* ΔCS cells expressing only SbtA7942
231 grew to similar or slightly higher densities compared to cells expressing SbtA7942 and tagged or
232 untagged SbtB7942 on solid media at pH 8 in air under a 12/12 h low light/dark regime (Fig. S8).This
233 suggests SbtB7942 is not essential for autotrophic growth of *Synechococcus* ΔCS and, consistent with
234 the photosynthetic performance (Fig. 5), is not required for optimal growth under these conditions.
235

236 **DISCUSSION**

237 Regulation of cyanobacterial bicarbonate transporters has been an unresolved question for
238 quite some time with patchy evidence for diverse mechanisms and co-factors that may be involved.
239 Here, we elucidated the potentially regulatory protein-protein interaction between two SbtA
240 bicarbonate transporters and their cognate PII-like SbtB proteins depend on the relative
241 concentrations of the adenylnucleotides ATP, ADP, AMP and cAMP. The SbtA-SbtB pairs originated
242 from the transitional α-cyanobacterium *Cyanobium sp.* PCC7001 and the ß- cyanobacterium
243 *Synechococcus elongatus* PCC7942 which are phylogenetically relatively distant species (Sánchez-
244 Baracaldo et al., 2019) and share limited overall sequence homology at the amino acid level, with
245 60% identity between the two SbtA (Fig. S9, S10) and 58% identity between the two SbtB (Fig. 7C,
246 S11) proteins, yet the interaction profiles for both SbtA-SbtB pairs were convincingly similar to
247 conclude both protein pairs share the same overall regulatory mechanisms.
248

249 **Is ATP or cAMP a primary effector?**

250 *In vivo*, the intracellular adenylnucleotide pools invariably contain ATP, ADP, AMP and cAMP,
251 albeit relative concentrations may vary rapidly dependent on metabolic activity in response to
252 environmental and developmental factors (De la Fuente et al., 2014). In cyanobacteria, cAMP is
253 predominantly a secondary messenger as part of different signalling events, whereas the relative
254 abundances of ATP, ADP and AMP pool defines the energy status of a cell. Notwithstanding, both
255 processes could translate Ci availability and Ci demand to SbtB-mediated regulation of SbtA. In
256 addition, relative abundance of cAMP, ATP and AMP in the adenylate pool are interdependently

257 influenced by the activities of adenylate cyclase and phosphodiesterases which catalyze cAMP
258 synthesis from ATP and hydrolytic degradation to AMP, respectively. Depending on the species,
259 adenylate cyclase activity is stimulated by N and P deficiency, osmotic stress, light quality and in
260 some cases also bicarbonate or CO_2 (Cann, 2004; Hammer et al., 2006; Xu and Su, 2009; Agostoni
261 and Montgomery, 2014), potentially linking cAMP and Ci sensing.
262 Evidence from *Synechocystis sp.* PCC6803 suggests the cAMP:AMP ratios determined formation of
263 SbtA:SbtB complexes and SbtA activity. The SbtB6803 protein from *Synechocystis* binds cAMP with
264 higher affinity than other adenylates, and was proposed to be a novel cAMP receptor sensing the Ci
265 status and mediating acclimation of the CCM to high Ci levels (Selim et al., 2018). High Ci acclimated
266 cells were characterized by elevated [cAMP], a high cAMP:AMP ratio and downregulated Ci uptake.
267 Under these conditions, SbtB6803 was dissociated from SbtA6803 which argued SbtA in the
268 unbound state was inactive. Conversely, bicarbonate uptake is upregulated in low Ci acclimated
269 cells, which coincided with a low cAMP:AMP ratio and high [AMP] favouring co-localization of SbtB
270 with SbtA in the membrane (Selim et al., 2018), and therefore suggested SbtA in the bound state
271 was active. These findings are difficult to reconcile with the simple interaction model based on SbtB-
272 mediated SbtA regulation in *E. coli*, where SbtA-dependent bicarbonate uptake measurement
273 consistently showed that SbtA alone was clearly active and co-expression of SbtA and SbtB
274 inactivated bicarbonate uptake, including the SbtA6803-SbtB6803, SbtA7001-SbtB7001 and
275 SbtA7942-SbtB7942 pairs (Du et al., 2014). The binding analyses performed here (Fig. 3) support the
276 view that low [ATP] and low AEC dominate association of SbtA7001-SbtB7001 and SbtA7942-
277 SbtB7942 pairs. We need to consider that the experimentally applied cAMP, but not ATP, ADP or
278 AMP concentrations, were almost certainly orders of magnitude higher than *in vivo* levels (Ohmori
279 and Okamoto, 2004). Therefore, it seems unlikely the intracellular [cAMP] required for effective
280 competition with [ATP], and thus affecting SbtA:SbtB binding, would occur under physiological
281 conditions. Species-related differences in cAMP-mediated regulation may provide a partial
282 explanation for differences between studies, such as the loss of cAMP receptor proteins (CRPs) from
283 the *Synechococcus elongatus* PCC7942 genome, amongst other *Prochlorococcus* and *Synechococcus*
284 species (Xu and Su, 2009). CRPs are transcriptional activators or repressors upon binding of cAMP,
285 involved in the regulation of multiple target genes. Possibly, roles of cAMP in post-translational
286 regulation, such as the interaction of SbtA7942 and SbtB7942, may also be affected. In addition, the
287 6-12 times higher binding affinity of ATP over cAMP, ADP or AMP to SbtB7001 (Kaczmarski et al.,
288 2019) as opposed to highest affinity for cAMP by SbtB6803 (Selim et al., 2018) suggests the
289 interaction of SbtB7001 and SbtA7001 may be more sensitive to the AEC.
290

291 **The SbtA and SbtB proteins interact dynamically in response to the adenylate energy charge**

292 Universally, ATP, ADP and AMP form the core of the energy system of living cells. The
293 majority of biochemically available energy is linearly correlated with the molar fraction of ATP and ½
294 molar fraction of ADP of the total adenylate pool, but was experimentally simplified by testing
295 effects of ATP:ADP and ATP:AMP ratio effects separately. Adenylate pools measured from a diverse
296 range of tissues, organisms and environmental conditions suggest active growth requires an energy
297 charge between 0.8 and 0.9, while a drop of the energy charge below 0.5 is unsustainable
298 (Chapman et al., 1971), which sets the expected response margins expected for AEC-regulated
299 processes. The AEC is often sensed by regulatory proteins through competitive binding of ATP or
300 ADP causing opposite directed responses (Atkinson and Walton, 1967). In fact, PII proteins have
301 been shown to sense the energy status of the cell and regulate target enzyme activity by undergoing
302 specific conformational changes in response to binding ATP or ADP which altered the interaction
303 between the PII protein and its target and modulated the activity of the target protein (Radchenko
304 et al., 2013; Zeth et al., 2014; Selim et al., 2019). This principle applied to binding of the PII-like SbtB
305 protein and SbtA from both cyanobacterial species investigated. The simulated AEC supporting more
306 than 90% unbound (and active) SbtA was 0.74 to 0.91 (Table 1), and corresponds well with the
307 measured ATP/(ATP+ADP) ratios of 0.8 in the light at pH 8 reported for a thermophile
308 *Synechococcus* strain (Kallas and Castenholz, 1982), 0.8 to 0.9 for *Synechococcus elongatus* (Rust et
309 al., 2011) and 0.8 for *Anacystis nidulans* (recalculated from (Bornefeld and Simonis, 1974)), which
310 suggests physiologically active cyanobacterial cells maintain an almost fully active pool of SbtA
311 protein dissociated from SbtB. This was corroborated by the *in vivo* activity of SbtA7942 in the
312 *Synechococcus* ΔCS strains expressing SbtA or both SbtA and SbtB, supporting the same
313 photosynthetic and bicarbonate uptake rates (Fig. 5, 6, S7) and growth at low Ci (Fig. S8). In
314 comparison, co-expression of SbtB and SbtA fully inhibited SbtA function in actively growing *E. coli*,
315 where all carbon sources had been removed prior to measuring bicarbonate uptake. This inhibition
316 had been attributed to the formation of SbtA:SbtB complexes (Du et al., 2014). If SbtA:SbtB
317 association was AEC-dependent, experimental conditions must have caused a sufficiently lower AEC
318 than 0.8, reported for *E. coli* in exponential growth phase (Chapman et al., 1971). One possibility is
319 that the high expression levels of a foreign membrane and soluble protein depleted internal energy
320 and N resources, and further removal of exogenous C sources led to stressed cells operating at a
321 substantially lower energy charge. Therefore, future analyses should explore whether artificially
322 raised intracellular [ATP] and AEC levels can dissociate SbtA:SbtB complexes and restore SbtA
323 activity in *E. coli* .
324

325 **Adenylnucleotide-dependent conformation of SbtB for regulatory interaction with SbtA**

326 In PII proteins the surface-exposed, flexible T-loop has been identified as the central region
327 that mediates the regulatory interaction of the PII protein with its target protein(s). The T-loop
328 undergoes ligand-induced conformation changes upon binding small effector molecules in a co-
329 operative or competitive manner which determines whether PII binds to its target. For example,
330 binding of ATP to the PII protein from *Synechococcus elongatus* PCC7942 induced T-loop
331 conformation changes facilitated association of N-acetyl-glutamate kinase (NAGK) and arginine
332 synthesis (Zeth et al., 2014; Selim et al., 2019), and the ADP-stabilized T-loop of the PII protein GlnK
333 from *E. coli* enable formation of an inactivating complex with the ammonium transporter AMTB
334 (Radchenko et al., 2010). There seems to be a direct correlation, analogous to PII proteins, between
335 changes to the flexible T-loop of SbtB7001 trimers ligands occupying the intermolecular nucleotide
336 binding clefts (Kaczmarski et al., 2019) and the opposing effects of ATP and ADP or AMP on
337 SbtA:SbtB binding and implicit SbtA regulation, which is summarized in Fig. 8. The probability for
338 each adenylate ligand to occupy a nucleotide binding site depends on the binding affinity and the
339 local concentration of the ligand. At high ATP:ADP or AMP ratios, when Ca^{2+}ATP occupies the
340 nucleotide binding sites of the SbtA trimers, the T-loops are stabilized through interactions of
341 specific residues with the γ-phosphate of ATP, in a position close to the core ('closed' conformation)
342 that limits further access to the site ((Kaczmarski et al., 2019), Fig. 7A). It appears that the Ca^{2+}ATP-
343 induced stable T-loop conformation prevents the SbtB7001 trimers from binding to SbtA, promoting
344 full SbtA activity. In contrast, at low ATP:ADP or AMP ratios, occupation of the binding site by ADP or
345 AMP leaves the T-loops in their inherent, disordered ('open') conformation ((Kaczmarski et al.,
346 2019), Fig. 7A), and SbtB is able to form a stable, inactivating complex with SbtA. The interaction
347 between SbtB7942 and SbtA7942 is likely to be modulated by a similar adenylnucleotide-induced T-
348 loop conformation change, inferred from highly homologous modelled structures of the two SbtB
349 proteins, their overall amino acid sequence identity of 57.7% and almost complete conservation of
350 the T-loop and ATP-binding residues (Fig. 7B, C). However, until the nature of the molecular
351 interactions between SbtB and SbtA are resolved, relationships between structure and function of
352 SbtB, particularly the T-loop, remain speculative.
353

354 **Implications for regulation of SbtA activity in cyanobacteria**

355 For cyanobacteria, it is a selective advantage to maximize photosynthetic CO_2 fixation and
356 carbon gain for growth in the light. In the dark, photosynthetic CO_2 fixation ceases making Ci
357 acquisition redundant and energetically futile. Additionally, continued accumulation of large
358 amounts of bicarbonate may disrupt intracellular pH and ion homeostasis, particularly if [Na^+] were

359 to build up by HCO_3^-/Na^+ symport due to SbtA activity. Therefore, the co-ordinated regulation of Ci
360 acquisition and photosynthetic activity may be imperative for survival and success of cyanobacteria.
361 A hypothetical scenario for the regulation of bicarbonate uptake by SbtA in cyanobacteria is
362 depicted in Fig. 8. SbtA and SbtB are both presented as trimers, which is supported by evidence from
363 crystal structures, size exclusion chromatography and homology to PII proteins for SbtB (Selim et al.,
364 2018; Kaczmarski et al., 2019), and is highly likely for SbtA (Du et al., 2014) but needs further
365 verification. We postulate two types of regulatory mechanisms for SbtA-mediated Ci uptake may
366 have evolved that differ in time scales, fast inactivation-activation within seconds to match rapid
367 changes in photosynthetic CO_2-fixation and longer-term inactivation as safe-guard against activation
368 under photosynthetically/metabolically unfavourable conditions which involves SbtB. In the light,
369 under low Ci conditions, bicarbonate uptake by SbtA may be limited by light intensity and substrate
370 availability, but SbtA functions independent of the SbtB protein (Fig. 5, S7). The AEC of the cell under
371 otherwise favourable environmental conditions would remain steady near 0.8 to 0.9 (Rust et al.,
372 2011), preventing SbtB from binding to SbtA. Upon onset of darkness, SbtA-mediated bicarbonate
373 transport is inactivated within seconds (Fig. 6). At this time scale involvement of SbtB is unrealistic.
374 Apart from evidence for SbtA inactivation in SbtB-less *Synechococcus*, inactivation is likely to occur
375 more quickly than the exchange of ATP for ADP or AMP from the SbtB trimers and subsequent
376 binding to SbtA even though the AEC may change rapidly. As shown for *Anacystis nidulans*, a dark-
377 induced drop in AEC can occur within seconds, reducing the ATP/(ATP+ADP) ratio from 0.85 to 0.4
378 and gradually stabilizing at about 0.6 after 30 minutes in the dark (calculated from (Bornefeld and
379 Simonis, 1974)). A similar immediate decline in ATP levels was observed in *Synechococcus* after a
380 light-to-dark shift, but ATP levels were restored to 85% of those in the light within 10 minutes
381 (Takano et al., 2015). In contrast, a one-hour lag in the dark was observed in *Synechococcus*
382 *elongatus* (Rust et al., 2011) before the ATP/(ATP+ADP) ratio decreased from 0.85 to 0.5. As such,
383 the nature of the fast signals and signal transduction pathways that trigger SbtA inactivation upon
384 the light-to-dark transition and, in reverse, its activation after dark-to-light remain virtually a black
385 box of unknowns (Fig. 8) with ample possibilities for speculation.
386 Light-dark transitions generate rapidly reversible changes in cellular redox status driven by
387 rapid photochemistry and physical properties of photosynthetic electron transport, known to
388 regulate CBB cycle enzyme activity via Chloroplast protein (CP)12 protein and ferredoxin-thioredoxin
389 system redox signalling cascades (Tamoi et al., 2005). It is intriguing to consider similar redox
390 regulation for SbtA. Although SbtA lacks highly conserved Cys residues that could form sulfhydryl
391 bonds with canonical CP12 or thioredoxins, a CP12 variant without sulfhydryl bonds identified in
392 *Synechococcus elongatus* PCC7942 may be a light and Ci responsive regulator. Gene expression of

393 the CP12 variant changed from high to low Ci conditions and with light intensity (Stanley et al.,
394 2013), and a deletion mutant exerted reduced growth under light-dark cycles (Tamoi et al., 2005).
395 Alternatively, potential redox-signalling may involve Ca^{2+}. Light-dark transitions produced specific,
396 short-lived 30 s [Ca^{2+}] spikes in the cyanobacterium *Anabaena sp.* PCC7120, which were suggested to
397 arise from influx of Ca^{2+} through plasma membrane located Ca^{2+} channels triggered by a redox
398 change within the photosynthetic electron transport chain (Torrecilla et al., 2004). Similarly, a dark-
399 induced change in membrane potential could have triggered opening of Ca^{2+} channels as observed in
400 phototaxis (Murvanidze and Glagolev, 1982) or the release of Ca^{2+} from the many Ca^{2+} binding
401 proteins present in cyanobacteria (Domínguez et al., 2015). A change in protein phosphorylation is
402 an efficient option for rapid regulatory post-translation modifications, illustrated by phospho-relays
403 able to transduce a stimulus into the motor response within 200 ms in regulation of chemotactic
404 motility in *E. coli* (Parkinson, 2003). The two major phospho-relay signal transduction systems are
405 two-component signalling systems and eukaryotic-type Ser/Thr and Tyr kinases and phosphatases.
406 Studies of cyanobacterial phospho-proteomes suggest extensive regulatory networks exist involving
407 phosphorylation cascades and relays for many biological processes, some of which combine two-
408 component signalling and Ser/Thr/Tyr phosphorylation (Dworkin, 2015). The extent of SbtA
409 phospho-regulation by light and Ci availability is unknown, but several highly conserved, cytoplasmic
410 exposed Ser, Thr, Tyr and Arg residues (Fig. S9) could be targets of redox and/or Ca^{2+} signalling-
411 coupled kinase-phosphatase systems, involving (i) light-dark/redox-responsive Ser, Thr or Tyr
412 phosphorylation/de-phosphorylation, (ii) Arg-phosphorylation by a redox/ Ca^{2+} sensory His kinase
413 analogous to two-component signalling, and (iii) a combination of phospho-transfer from a sensory
414 His kinase to a Ser/Thr or Tyr kinase/phosphatase acting on SbtA.
415 The relatively longer time constants for binding of SbtB to SbtA, exceeding initial SbtA
416 inactivation, and the AEC-dependence involved in SbtB-mediated SbtA regulation, clearly favour a
417 role for SbtB as "curfew" protein in longer-term inactivation of SbtA. Depending on the analysis, the
418 cellular adenylate energy charge dropped to about 0.6 within minutes to an hour in the dark. Based
419 on the *in vitro* binding analyses (this work), this AEC is sufficiently low to replace ATP with ADP and
420 AMP in the nucleotide binding sites in SbtB trimers and to sequester substantial amounts of SbtA
421 into stable inactive complexes. The stoichiometry of SbtA and SbtB trimers within complexes
422 remains to be elucidated. The association with SbtB shields SbtA from fast re-activation and would
423 overwrite any environmental and intrinsic cues that may otherwise induce futile
424 activation/inactivation cycles and activation of SbtA under conditions causing pro-longed inhibition
425 of photosynthetic CO_2 assimilation such as darkness and a low AEC at night. In addition, there may
426 be conditions requiring stable inactivation of SbtA in the light during prolonged nutrient or

427 environmental stress energy if the AEC falls significantly below 0.8 and resources are invested in
428 protective processes instead of photosynthesis and Ci accumulation. After transition from dark to
429 light the AEC rises very rapidly and bicarbonate uptake is activated after about 30 s (Badger and
430 Andrews, 1982). This suggests the majority of the SbtA:SbtB complexes must dissociate within this
431 time frame for SbtA to be active. It is conceivable that the 6-12 times higher binding affinity of ATP
432 to SbtB7001 and greater ease of access to the nucleotide binding site with ADP or AMP bound
433 facilitate a more rapid replacement of the low affinity ligands ADP and AMP by ATP than in reverse.
434

435 **Conclusions**

436 The interactions of the SbtB7001 and SbtB7942 proteins with their corresponding SbtA
437 bicarbonate transporters are the first examples among PII-like proteins that provide evidence for
438 SbtB as a sensor and regulatory protein in response to the adenylate energy charge of the cell,
439 similar to canonical PII proteins. The two SbtA-SbtB pairs used here appear to be subject to the same
440 adenylnucleotide regulation despite their origin from two distinct genera, *Cyanobium* and
441 *Synechococcus*. It will be of interest to assess SbtA-SbtB interactions across a wide range of species
442 to evaluate to which extent AEC-mediated regulation has been adopted across cyanobacterial
443 species. The light-dark regulation of SbtA *in vivo* raises many questions. The light signalling
444 pathway(s) and the molecular mechanism(s), independent of SbtB, need to be addressed, perhaps
445 with redox- and post-translational regulation of SbtA as a starting point for further investigations.
446 Likewise, the basis of energy charge-sensing of SbtB and its interaction with SbtA is clear, though the
447 precise details are far from being fully understood. The elucidation of molecular and biochemical
448 mechanisms underlying the interaction between SbtA and SbtB, causality of AEC and SbtA:SbtB
449 complex formation *in vivo* and differential effects of environmental conditions are challenges for the
450 future. However, the link between SbtB as a sensor of the cellular energy status and response
451 regulator of SbtA activity is an important insight which aids informed strategies for expression of the
452 SbtA-SbtB systems from *Synechococcus* and *Cyanobium* in higher plant chloroplasts.
453

454 **MATERIALS AND METHODS**

455 Detailed information on protocols and materials are provided as Supplementary Information.

456 ***E. coli* and cyanobacterial cell lines**

457 Nucleotide and amino acid sequences are referred to by gene ID and Locus_tags from IMG
458 (Integrated Microbial Genome database; https://img.jgi.doe.gov). The HCO_3^- uptake deficient cell
459 line *Synechococcus* ΔCS was derived from wild-type *Synechococcus elongatus* PCC794 by eliminating

460 expression of the bicarbonate transporters BCT1 and SbtA. The *cmpA* (IMG ID: 637799921,
461 Synpcc7942_1488) and *cmpB* (IMG ID: 637799922, Synpcc7942_1489) genes were inactivated with a
462 kanamycin resistance (*kan*^{R}) marker (Omata et al., 1999), and both the *sbtA* (IMG ID: 637799907,
463 Synpcc7942_1475) and *sbtB* (IMG ID: 637799908, Synpcc7942_1476) genes were replaced with a
464 chloramphenicol resistance (*cm*^{R}) gene (Dzelzkalns et al., 1984) (Table 1). For protein expression,
465 *sbtA* and *sbtB* genes from *Synechococcus elongatus* PCC7942 and *Cyanobium sp.* PCC7001 (IMG ID:
466 647590134, CPCC7001_1784 and IMG ID: 647590133, CPCC7001_1671, respectively) were
467 synthesized (GenScript, New Jersey, USA) and inserted into plasmids pSE2-1 and pSE4-1 carrying a
468 spectinomycin resistance (*sp*^{R}) marker (Price et al., 2004; Du et al., 2014). Gene expression is
469 controlled by under the isopropyl β-D-1-thiogalactopyranoside (IPTG)-inducible *lacZ* promoter in
470 pSE2-1 and native *sbtA* and *sbtB* promoters in pSE4-1. The SbtB proteins were C-terminally tagged
471 with a HAHis epitope for immunodetection and affinity purification. For a full list of cell lines and
472 expression vectors refer to Table S2.
473
474 **Growth of *E. coli* and cyanobacteria**
475 For maintenance, mutant selection and protein expression, *E. coli* DH5α derived cell lines
476 were grown in Lysogeny broth (LB; sp100 µg ml^{-1}) as described (Du et al., 2014). Expression of SbtA
477 and SbtB proteins was induced for 3 h with 1 mM IPTG in *E. coli*. *Synechococcus* ΔCS cell lines were
478 grown in modified BG-11 medium buffered with 20 mM HEPES-KOH pH 8.0 (Maeda et al., 2002;
479 Woodger et al., 2003) in high Ci (2-4% (v/v) CO_2 enriched air) or low Ci (ambient air, 400 ppm CO_2)
480 conditions under constant light (70 µmol m^{-2} s^{-1}). Antibiotics were supplied as appropriate (kan 100
481 µg ml^{-1}, cm 8 µg ml^{-}1, sp 100 µg ml^{-1}). Protein expression of SbtA and SbtB was induced by exposing
482 high Ci-grown for 4 h to low Ci. For growth assays, a dilution series of low Ci-induced cultures were
483 spotted onto agar plates and grown in air under 12 h light (50 µmol m^{-2} s^{-1})/12 h dark cycles.
484
485 **Extraction of native proteins**
486 The isolation of membrane-enriched fractions of native proteins from *E. coli* and
487 cyanobacteria was adapted from (Du et al., 2014). Membrane proteins were resuspended in IMAC
488 HEPES binding buffer (50 mM HEPES, 100 mM NaCl, 25 M imidazole, pH 8.0) supplemented with 1%
489 (w/v) *n*-Dodecyl β-D-maltoside (DDM) for further analysis.
490
491 **Immobilized metal affinity chromatography (IMAC) protein binding assays and quantification of**
492 **SbtA:SbtB binding**

493 The association of SbtA and HAHis-tagged SbtB proteins was analysed in IMAC binding
494 assays adapted from (Du et al., 2014). Native protein extracts were incubated in IMAC HEPES binding
495 buffer supplemented with 200 nM $CaCl_2$ and a range of potential effector molecules, and Ni-charged
496 Profinity™ IMAC resin (Biorad, USA) for 1 h at 23 °C to allow HAHis-tagged SbtB to bind to the resin
497 and SbtA to associate with SbtB. Details on effectors and adenylnucleotide ratios are provided in the
498 figures and captions. IMAC purified SbtA:SbtB complexes were subjected to immunoblot analysis as
499 described in (Du et al., 2014). SbtA protein was quantified by densitometry of Western blot images
500 (ImageLab software (BioRad, USA) and correlated with the adenylnucleotide ratio (AR) in the binding
501 reaction. The AR corresponding to 50% (AR_{50}), 25% (AR_{25}) and 10% (AR_{10}) of SbtA associated with
502 SbtA:SbtB complexes were estimated from sigmoidal logistic curve fits (OriginPro v2020, OriginLab
503 Corp., USA).
504
505 **Photosynthetic analysis by membrane inlet mass spectrometry (MIMS) measurements**
506 Net photosynthetic O_2 evolution and Ci uptake rates were calculated from changes in the
507 concentrations of dissolved CO_2 and O_2 in low Ci induced cyanobacterial cell suspensions measured
508 in a closed cuvette attached to a mass spectrometer as described previously (Badger and Andrews,
509 1982; Badger et al., 1985, Price, 2004 #32). CO_2 uptake was inhibited with 500 µM EZ and HCO_3^--
510 dependent photosynthetic O_2 evolution rates determined after incremental additions of bicarbonate
511 with cell densities of 4 µg ml^{-1} chlorophyll *a* (Chl *a*). Chl *a* content was determined
512 spectrophotometrically in 90% (v/v) methanol extracts (Porra et al., 1989). Maximum velocity of O_2
513 evolution (V_{max}) and affinity for HCO_3^- ($k_{0.5}$) were derived from Michaelis-Menten kinetics.
514
515 **Ci uptake measurement by silicon oil centrifugation-filtration**
516 Light- and dark stimulated uptake of active species of $[^{14}C]HCO_3^-$ in cyanobacterial cell
517 cultures was measured by using the silicon oil centrifugation-filtration method as described
518 previously (Kaplan et al., 1980; Price and Badger, 1989). Low Ci-induced cell cultures at cell densities
519 equal to 4 µg ml^{-1} Chl *a* were treated with 500 µM EZ, and $[^{14}C]HCO_3^-$ uptake determined for a 30 s-
520 interval at various time points after a light to dark shift. HCO_3^- uptake rates were calculated based on
521 the specific activity of the $[^{14}C]HCO_3^-$ substrate.
522
523 **Bioinformatics**
524 Homologous SbtA and SbtB proteins were identified in BLASTP (Altschul et al., 1990)
525 searches and multiple pairwise amino acid sequence alignments generated in Geneious Prime
526 2020.2.4 (https://www.geneious.com) with MUSCLE software (Edgar, 2004). Protein identifiers are

527 the gene IDs and Locus_tags from IMG (further detail in Tables S3 and S4). The domain homology
528 model of the SbtB7942 monomer was generated in PSIPRED workbench
529 (http://bioinf.cs.ucl.ac.uk/psipred/) and the fully automated homology modelling workflow Domserf
530 2.1 (Buchan and Jones, 2019). Template models were identified from PSI BLAST searches against the
531 PDB and CATH databases and parsed into domains for optimal matching against the query sequence.
532 Final models were constructed by MODELLER software based on a subset of best domain matches to
533 SbtB7942. The overall folds of SbtB7942 and SbtB7001 chain A with ADP (PDB ID: 6MMC) or Ca^{2+} and
534 ATP ligands (PDB ID: 6MM2) proteins were compared by superimposition, using Chimera v1.14
535 (http://www.cgl.ucsf.edu/chimera) and MatchMaker (Meng et al., 2006).
536
537 **Statistics**
538 Statistically significant differences between data sets were determined by performing a one-
539 way analysis of variance (ANOV) and post-hoc Tukey's Honest Significant Difference (HSD) test
540 (Tukey, 1949), using a type I error level α=0.05 as threshold ($P < 0.05$).
541

542 **ACKNOWLEDGEMENTS**
543 This work was supported by the Australian Government through the Australian Research
544 Council Centre of Excellence for Translational Photosynthesis (CE1401000015). J.A.K. acknowledges
545 support from an Australian Government Research Training Program Scholarship.
546

547 **REFERENCES**

548 **Agostoni M, Montgomery BL** (2014) Survival strategies in the aquatic and terrestrial world: The
549 impact of second messengers on cyanobacterial processes. Life **4:** 745-769
550 **Altschul SF, Gish W, Miller W, Myers EW, Lipman DJ** (1990) Basic local alignment search tool.
551 Journal of Molecular Biology **215:** 403-410
552 **Atkinson DE, Walton GM** (1967) Adenosine triphosphate conservation in metabolic regulation: Rat
553 liver citrate cleavage enzyme. Journal of Biological Chemistry **242:** 3239-3241
554 **Badger MR, Andrews TJ** (1982) Photosynthesis and inorganic carbon usage by the marine
555 cyanobacterium, synechococcus sp. Plant Physiology **70:** 517-523
556 **Badger MR, Bassett M, Comins HN** (1985) A model for HCO_3^- accumulation and photosynthesis in
557 the cyanobacterium *Synechococcus sp*: Theoretical predictions and experimental
558 observations. Plant Physiology **77:** 465-471
559 **Badger MR, Price GD** (1992) The CO_2concentrating mechanism in cyanobactiria and microalgae.
560 Physiologia Plantarum **84:** 606-615
561 **Bornefeld T, Simonis W** (1974) Effects of light, temperature, pH, and inhibitors on the ATP level of
562 the blue-green alga *Anacystic nidulans*. Planta **115:** 309-318
563 **Buchan DWA, Jones DT** (2019) The PSIPRED protein analysis workbench: 20 years on. Nucleic Acids
564 Research **47:** W402-W407
565 **Cann M** (2004) Bicarbonate stimulated adenylyl cyclases. IUBMB Life **56:** 529-534

Chapman AG, Fall L, Atkinson DE (1971) Adenylate energy charge in *Escherichia coli* during growth and starvation. Journal of Bacteriology **108:** 1072-1086

De la Fuente IM, Cortés JM, Valero E, Desroches M, Rodrigues S, Malaina I, Martínez L (2014) On the dynamics of the adenylate energy system: homeorhesis vs homeostasis. PLOS ONE **9:** e108676

Domínguez DC, Guragain M, Patrauchan M (2015) Calcium binding proteins and calcium signaling in prokaryotes. Cell Calcium **57:** 151-165

Du J, Förster B, Rourke L, Howitt SM, Price GD (2014) Characterisation of cyanobacterial bicarbonate transporters in *E. Coli* shows that Sbta homologs are functional in this heterologous expression system. PLoS ONE **9:** e115905

Dworkin J (2015) Ser/Thr phosphorylation as a regulatory mechanism in bacteria. Current Opinion in Microbiology **24:** 47-52

Dzelzkalns VA, Owens GC, Bogorad L (1984) Chloroplast promoter driven expression of the chloramphenicol acetyl transferase gene in a cyanobacterium. Nucleic acids research **12:** 8917-8925

Edgar RC (2004) MUSCLE: a multiple sequence alignment method with reduced time and space complexity. BMC Bioinformatics **5:** 113

Espie G, Kimber M (2011) Carboxysomes: cyanobacterial RubisCO comes in small packages. Photosynthesis Research **109:** 7-20

Field CB, Behrenfeld MJ, Randerson JT, Falkowski P (1998) Primary production of the biosphere: Integrating terrestrial and oceanic components. Science **281:** 237-240

Forchhammer K, Lüddecke J (2016) Sensory properties of the PII signalling protein family. The FEBS Journal **283:** 425-437

Hammer A, Hodgson DRW, Cann MJ (2006) Regulation of prokaryotic adenylyl cyclases by CO2. The Biochemical Journal **396:** 215-218

Huergo LF, Chandra G, Merrick M (2013) PII signal transduction proteins: nitrogen regulation and beyond. FEMS Microbiology Reviews **37:** 251-283

Huergo LF, Dixon R (2015) The emergence of 2-oxoglutarate as a master regulator metabolite. Microbiology and Molecular Biology Reviews **79:** 419-435

Kaczmarski JA, Hong N-S, Mukherjee B, Wey LT, Rourke L, Förster B, Peat TS, Price GD, Jackson CJ (2019) Structural basis for the allosteric regulation of the SbtA bicarbonate transporter by the PII-like protein, SbtB, from *Cyanobium sp.* PCC7001. Biochemistry **58:** 5030-5039

Kallas T, Castenholz RW (1982) Internal pH and ATP-ADP pools in the cyanobacterium *Synechococcus sp.* during exposure to growth-inhibiting low pH. Journal of Bacteriology **149:** 229-236

Kaplan A, Badger M, Berry J (1980) Photosynthesis and the intracellular inorganic carbon pool in the bluegreen alga *Anabaena variabilis*: Response to external CO_2 concentration. Planta **149:** 219-226

Kaplan A, Reinhold L (1999) Co2 concentrating mechanisms in photosynthetic microorganisms. Annual Review of Plant Physiology and Plant Molecular Biology **50:** 539-570

Kaplan A, Zenvirth D, Marcus Y, Omata T, Ogawa T (1987) Energization and activation of inorganic carbon uptake by light in cyanobacteria. Plant Physiology **84:** 210-213

Leganés F, Forchhammer K, Fernández-Piñas F (2009) Role of calcium in acclimation of the cyanobacterium *Synechococcus elongatus* PCC 7942 to nitrogen starvation. Microbiology **155:** 25-34

Liu H, Nolla H, Campbell L (1997) Prochlorococcus growth rate and contribution to primary production in the equatorial and subtropical North Pacific Ocean. Aquatic Microbial Ecology **12:** 39-47

Long BM, Rae BD, Rolland V, Förster B, Price GD (2016) Cyanobacterial CO_2-concentrating mechanism components: function and prospects for plant metabolic engineering. Current Opinion in Plant Biology **31:** 1-8

Maeda S-i, Badger MR, Price GD (2002) Novel gene products associated with NdhD3/D4-containing NDH-1 complexes are involved in photosynthetic CO_2 hydration in the cyanobacterium, *Synechococcus sp.* PCC7942. Molecular Microbiology **43:** 425-435

McGinn PJ, Price GD, Maleszka R, Badger MR (2003) Inorganic carbon limitation and light control the expression of transcripts related to the CO_2-concentrating mechanism in the cyanobacterium *Synechocystis sp.* strain PCC6803. Plant Physiology **132:** 218-229

McGrath JM, Long SP (2014) Can the cyanobacterial carbon-concentrating mechanism increase photosynthesis in crop species? A theoretical analysis. Plant Physiology **164:** 2247-2261

Meng EC, Pettersen EF, Couch GS, Huang CC, Ferrin TE (2006) Tools for integrated sequence-structure analysis with UCSF Chimera. BMC bioinformatics **7:** 339-339

Meyer MT, McCormick AJ, Griffiths H (2016) Will an algal CO_2-concentrating mechanism work in higher plants? Current Opinion in Plant Biology **31:** 181-188

Murvanidze GV, Glagolev AN (1982) Electrical nature of the taxis signal in cyanobacteria. Journal of Bacteriology **150:** 239-244

Ogawa T, Miyano A, Inoue Y (1985) Photosystem-I-driven inorganic carbon transport in the cyanobacterium, Anacystis nidulans. Biochimica et Biophysica Acta (BBA) - Bioenergetics **808:** 77-84

Ohkawa H, Sonoda M, Hagino N, Shibata M, Pakrasi HB, Ogawa T (2002) Functionally distinct NAD(P)H dehydrogenases and their membrane localization in *Synechocystis sp*. PCC6803. Functional Plant Biology **29:** 195-200

Ohmori M, Okamoto S (2004) Photoresponsive cAMP signal transduction in cyanobacteria. Photochemical & Photobiological Sciences **3:** 503-511

Omata T, Price GD, Badger MR, Okamura M, Gohta S, Ogawa T (1999) Identification of an ATP-binding cassette transporter involved in bicarbonate uptake in the cyanobacterium *Synechococcus sp.* strain PCC 7942. Proceedings of the National Academy of Sciences **96:** 13571-13576

Parkinson JS (2003) Bacterial chemotaxis: A new player in response regulator dephosphorylation. Journal of Bacteriology **185:** 1492-1494

Porra RJ, Thompson WA, Kriedemann PE (1989) Determination of accurate extinction coefficients and simultaneous equations for assaying chlorophylls a and b extracted with four different solvents: verification of the concentration of chlorophyll standards by atomic absorption spectroscopy. Biochimica et Biophysica Acta (BBA) - Bioenergetics **975:** 384-394

Price G (2011) Inorganic carbon transporters of the cyanobacterial CO_2 concentrating mechanism. Photosynthesis Research **109:** 47-57

Price GD, Badger MR (1989) Ethoxyzolamide inhibition of CO_2 uptake in the cyanobacterium *Synechococcus* PCC7942 without apparent inhibition of internal carbonic anhydrase activity. Plant Physiology **89:** 37-43

Price GD, Badger MR (1989) Isolation and characterization of high CO_2-requiring-mutants of the cyanobacterium *Synechococcus* PCC7942: Two phenotypes that accumulate inorganic carbon but are apparently unable to generate CO_2 within the carboxysome. Plant Physiology **91:** 514-525

Price GD, Badger MR, Woodger FJ, Long BM (2008) Advances in understanding the cyanobacterial CO_2-concentrating-mechanism (CCM): functional components, Ci transporters, diversity, genetic regulation and prospects for engineering into plants. Journal of Experimental Botany **59:** 1441-1461

Price GD, Pengelly JJL, Forster B, Du J, Whitney SM, von Caemmerer S, Badger MR, Howitt SM, Evans JR (2013) The cyanobacterial CCM as a source of genes for improving photosynthetic CO_2 fixation in crop species. Journal of Experimental Botany **64:** 753-768

Price GD, Shelden MC, Howitt SM (2011) Membrane topology of the cyanobacterial bicarbonate transporter, SbtA, and identification of potential regulatory loops. Molecular Membrane Biology **28:** 265-275

668 **Price GD, Woodger FJ, Badger MR, Howitt SM, Tucker L** (2004) Identification of a SulP-type
669 bicarbonate transporter in marine cyanobacteria. Proceedings of the National Academy of
670 Sciences **101:** 18228-18233
671 **Radchenko MV, Thornton J, Merrick M** (2010) Control of AmtB-GlnK complex formation by
672 intracellular levels of ATP, ADP, and 2-oxoglutarate. The Journal of Biological Chemistry **285:**
673 31037-31045
674 **Radchenko MV, Thornton J, Merrick M** (2013) P_{II} signal transduction proteins are ATPases whose
675 activity is regulated by 2-oxoglutarate. Proceedings of the National Academy of Sciences
676 **110:** 12948-12953
677 **Rae BD, Förster B, Badger MR, Price GD** (2011) The CO_2-concentrating mechanism of *Synechococcus*
678 WH5701 is composed of native and horizontally-acquired components. Photosynthesis
679 Research **109:** 59-72
680 **Rath A, Glibowicka M, Nadeau VG, Chen G, Deber CM** (2009) Detergent binding explains anomalous
681 SDS-PAGE migration of membrane proteins. Proceedings of the National Academy of
682 Sciences **106:** 1760-1765
683 **Rust MJ, Golden SS, O'Shea EK** (2011) Light-driven changes in energy metabolism directly entrain
684 the cyanobacterial circadian oscillator. Science **331:** 220-223
685 **Sánchez-Baracaldo P, Bianchini G, Di Cesare A, Callieri C, Chrismas NAM** (2019) Insights into the
686 evolution of picocyanobacteria and phycoerythrin genes (*mpeBA* and *cpeBA*). Frontiers in
687 Microbiology **10:** 45
688 **Schwarz D, Nodop A, Hüge J, Purfürst S, Forchhammer K, Michel K-P, Bauwe H, Kopka J, Hagemann**
689 **M** (2011) Metabolic and transcriptomic phenotyping of inorganic carbon acclimation in the
690 cyanobacterium *Synechococcus elongatus* PCC 7942. Plant Physiology **155:** 1640-1655
691 **Selim KA, Haase F, Hartmann MD, Hagemann M, Forchhammer K** (2018) P_{II}-like signaling protein
692 SbtB links cAMP sensing with cyanobacterial inorganic carbon response. Proceedings of the
693 National Academy of Sciences **115:** E4861-E4869
694 **Selim KA, Haffner M, Watzer B, Forchhammer K** (2019) Tuning the in vitro sensing and signaling
695 properties of cyanobacterial PII protein by mutation of key residues. Scientific Reports **9:**
696 18985
697 **Shibata M, Katoh H, Sonoda M, Ohkawa H, Shimoyama M, Fukuzawa H, Kaplan A, Ogawa T** (2002)
698 Genes essential to sodium-dependent bicarbonate transport in cyanobacteria. Journal of
699 Biological Chemistry **277:** 18658-18664
700 **Stanley DN, Raines CA, Kerfeld CA** (2013) Comparative analysis of 126 cyanobacterial genomes
701 reveals evidence of functional diversity among homologs of the redox-regulated CP12
702 protein. Plant Physiology **161:** 824-835
703 **Sültemeyer D, Klughammer B, Badger MR, Dean Price G** (1998) Fast induction of high-affinity HCO_3^-
704 transport in cyanobacteria. Plant Physiology **116:** 183-192
705 **Takano S, Tomita J, Sonoike K, Iwasaki H** (2015) The initiation of nocturnal dormancy in
706 Synechococcus as an active process. BMC Biology **13:** 36
707 **Tamoi M, Miyazaki T, Fukamizo T, Shigeoka S** (2005) The Calvin cycle in cyanobacteria is regulated
708 by CP12 via the NAD(H)/NADP(H) ratio under light/dark conditions. The Plant Journal **42:**
709 504-513
710 **Thauer RK, Jungermann K, Decker K** (1977) Energy conservation in chemotrophic anaerobic
711 bacteria. Bacteriological Reviews **41:** 100-180
712 **Torrecilla I, Leganés F, Bonilla I, Fernández-Piñas F** (2004) Light-to-dark transitions trigger a
713 transient increase in intracellular Ca^{2+} modulated by the redox state of the photosynthetic
714 electron transport chain in the cyanobacterium *Anabaena sp.* PCC7120. Plant, Cell &
715 Environment **27:** 810-819
716 **Tukey JW** (1949) Comparing individual means in the analysis of variance. Biometrics **5:** 99-114
717 **Wheatley NM, Eden KD, Ngo J, Rosinski JS, Sawaya MR, Cascio D, Collazo M, Hoveida H, Hubbell**
718 **WL, Yeates TO** (2016) A PII-like protein regulated by bicarbonate: Structural and biochemical

719 studies of the carboxysome-associated CPII protein. Journal of Molecular Biology **428:** 4013-
720 4030
721 **Woodger FJ, Badger MR, Price GD** (2003) Inorganic carbon limitation induces transcripts encoding
722 components of the CO_2-concentrating mechanism in *Synechococcus sp.* PCC7942 through a
723 redox-independent pathway. Plant Physiology **133:** 2069-2080
724 **Xu M, Su Z** (2009) Computational prediction of cAMP receptor protein (CRP) binding sites in
725 cyanobacterial genomes. BMC Genomics **10:** 23
726 **Yaginuma H, Kawai S, Tabata KV, Tomiyama K, Kakizuka A, Komatsuzaki T, Noji H, Imamura H**
727 (2014) Diversity in ATP concentrations in a single bacterial cell population revealed by
728 quantitative single-cell imaging. Scientific reports **4:** 6522-6522
729 **Zeth K, Fokina O, Forchhammer K** (2014) Structural basis and target-specific modulation of ADP
730 sensing by the *Synechococcus elongatus* PII signaling protein. The Journal of Biological
731 Chemistry **289:** 8960-8972

732

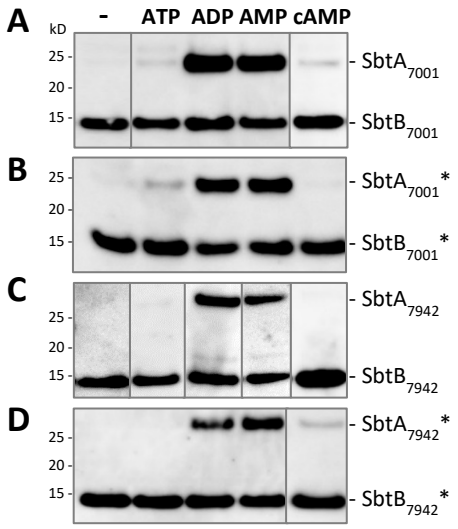

Fig. 1. Effects of adenylnucleotides on the association of SbtA and cognate SbtB proteins. The SbtA7001-SbtB7001 and SbtA7942-SbtB7942 pairs were expressed in *E. coli* (**A, C**) and *Synechococcus* ΔCS (*; **B, D**). During *in vitro* IMAC binding assays with 2 mM ATP, ADP, AMP, or cAMP, the HAHis-tagged SbtB proteins were immobilized for interaction with SbtA proteins and effectors. The SbtB protein and corresponding amounts of SbtA retained in SbtA:SbtB complexes were detected immunologically. The composite Western blot image is representative; n=3-8 per adenylnucleotide treatment.

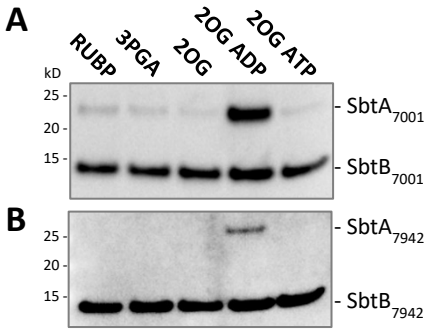

Fig. 2. The association of SbtA and cognate SbtB proteins is not linked to key metabolites of the CBB cycle, RUBP and 3PGA, and the TCA cycle, 2OG. The SbtA7001-SbtB7001 (**A**) and SbtA7942-SbtB7942 (**B**) pairs were expressed in *E. coli*. *In vitro* IMAC binding assays were performed with 2 mM RUBP, 3PGA or 2OG, and 2 mM 2OG and 2 mM ADP, or ATP combined (2OG ADP and 2OG ATP, respectively). The HAHis-tagged SbtB proteins and the SbtA proteins retained in SbtA:SbtB complexes were detected immunologically. Representative Western blot images; n=2.

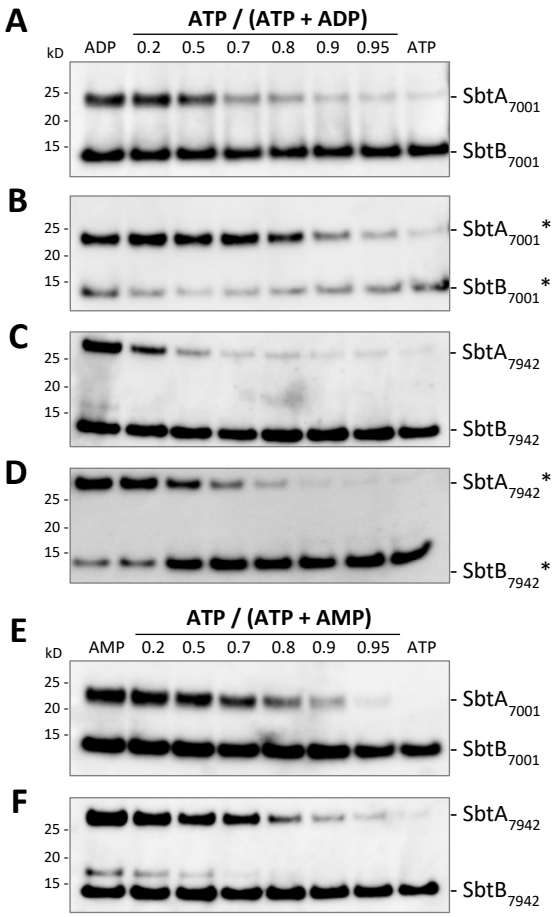

Fig. 3. Effects of ATP:ADP and ATP:AMP ratios on the association of SbtA and SbtB proteins. The SbtA7001-SbtB7001 (**A, C, E**) and SbtA7942-SbtB7942 (**B, D, F**) pairs were expressed in *E. coli* (**A, C, E, F**) and in *Synechococcus* ΔCS (*; **B, D**). Variation in energy charge was simulated in *in vitro* IMAC binding assays by different molar ratios of ATP:ADP (**A-D**) and ATP:AMP (**E, F**), with the total adenylnucleotide concentration at 2 mM. The HAHis-tagged SbtB proteins and the SbtA proteins retained in SbtA:SbtB complexes were detected immunologically. The 17 kD-protein above SbtB7942 is a fragment specific to SbtA. Representative Western blot images; n=3-4 per adenylnucleotide treatment.

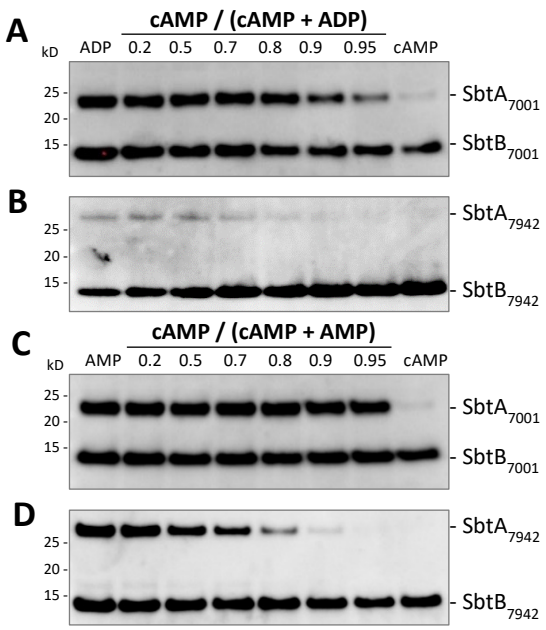

Fig. 4. Effects of the cAMP:ADP and cAMP:AMP ratios on the association of SbtA and SbtB proteins. The SbtA7001-SbtB7001 (**A, C**) and SbtA7942-SbtB7942 (**B, D**) pairs were expressed in *E. coli*. *In vitro* IMAC binding assays were performed with a range of cAMP:ADP (**A, B**) and cAMP:AMP (**C, D**) ratios, with a total adenylnucleotide concentration of 2 mM. The HAHis-tagged SbtB proteins and the SbtA proteins retained in SbtA:SbtB complexes were detected immunologically. Representative Western blot images; n=3 per adenylnucleotide treatment.

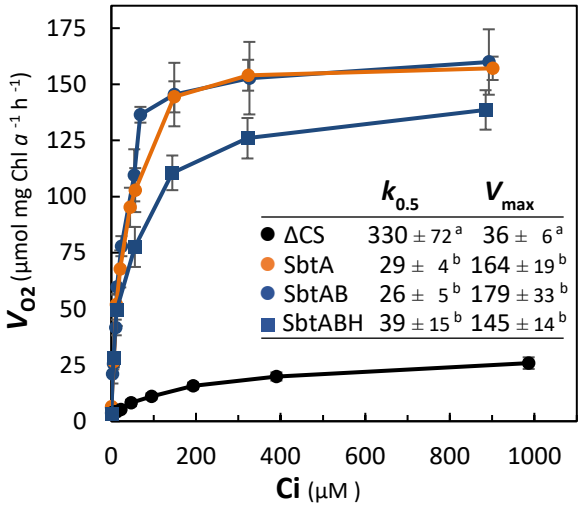

Fig. 5. Net photosynthetic O_2 evolution rates of *Synechococcus* ΔCS supported by SbtA-dependent bicarbonate uptake in the presence and absence of SbtB. The SbtA7942 protein was expressed without SbtB7942 (SbtA) or with untagged (SbtAB) or HAHis-tagged SbtB7942 (SbtABH) from plasmids in low Ci induced *Synechococcus* ΔCS. Steady state photosynthetic O_2 evolution rates (V_{O2}) were determined over a range of external Ci concentrations, while CO_2 uptake was inhibited by EZ, with MIMS. Maximum O_2 evolution rates (V_{max}, µmol mg Chl a^{-1} h^{-1}) and the Ci concentrations required for half-maximum photosynthetic rates ($k_{0.5}$, µM) were derived from Michaelis-Menten kinetics (inset). Statistically significant differences ($P < 0.05$) are indicated by different letters. Values are means ± SE; n=11 (ΔCS), n=9 (SbtA), n=7 (SbtAB), n=3 (SbtABH).

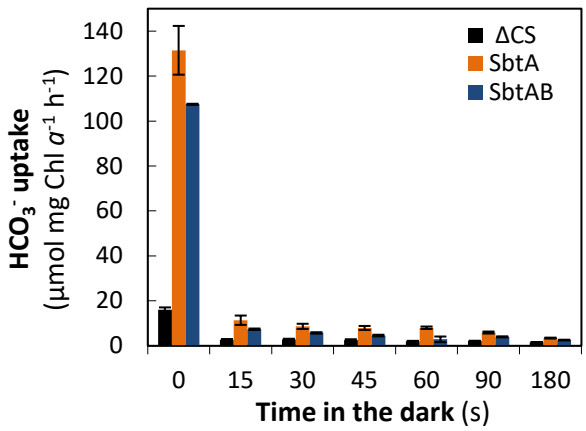

Fig. 6. Dark-inactivation of SbtA-mediated bicarbonate uptake in *Synechococcus* ΔCS in the presence and absence of SbtB. Bicarbonate transport activity of SbtA7942 was estimated from the accumulation of ^{14}C in *Synechococcus* ΔCS cells after silicon oil centrifugation-filtration. Gross HCO_3^- uptake rates normalized to Chl *a* content are shown at various time points following a shift from light into the dark for SbtA7942 only (SbtA) and SbtA7942 co-expressed with SbtB7942 (SbtAB). Residual HCO_3^- uptake rates for ΔCS represent passive, intracellular ^{14}C accumulation and extracellular ^{14}C trapped in the water shell adhering to each cell. Values are means ± SE; n=3-5.

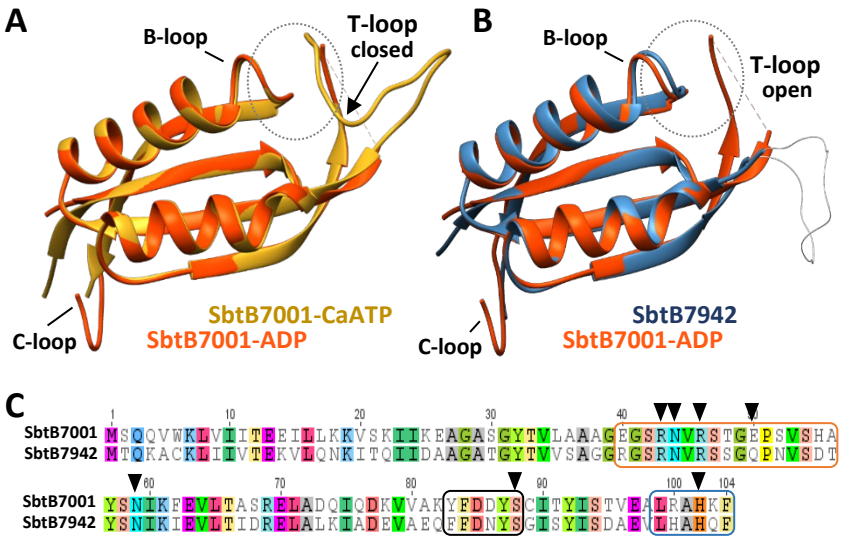

Fig 7. Structural comparison of the overall fold of SbtB7942 and SbtB7001 protein models. (**A**) Superimposition of the three-dimensional models derived from crystal structures of SbtB7001 with Ca^{2+} and ATP ligands (SbtB7001-CaATP; PDB ID 6MM2) and SbtB7001 binding ADP (SbtB7001-ADP; PDB ID 6MMC). The grey circles indicate the location of the nucleotide binding cleft. Ligand-induced structural differences affect primarily the T-loop which assumed a closed conformation in SbtB7001-CaATP and an open, disordered state in SbtB7001-ADP. (**B**) Superimposition the PSIPRED generated domain homology model of the apo-SbtB7942 monomer on the SbtB7001-ADP structure. The core structures of both SbtB proteins are highly similar, independent of ligands bound to SbtB7001. The configuration of the T-loop of SbtB7942 (grey coil) was modelled without ligand present. Therefore the open state was assumed. (**C**) Pairwise amino acid sequence alignment of SbtB7001 and SbtB7942 (57.7 % identity). Identical residues are highlighted in colour. The T-, B- and C-loop residues are framed orange, black and blue, respectively. Black arrows indicate critical residues for binding ATP phosphate groups (Kaczmarski et al., 2019).

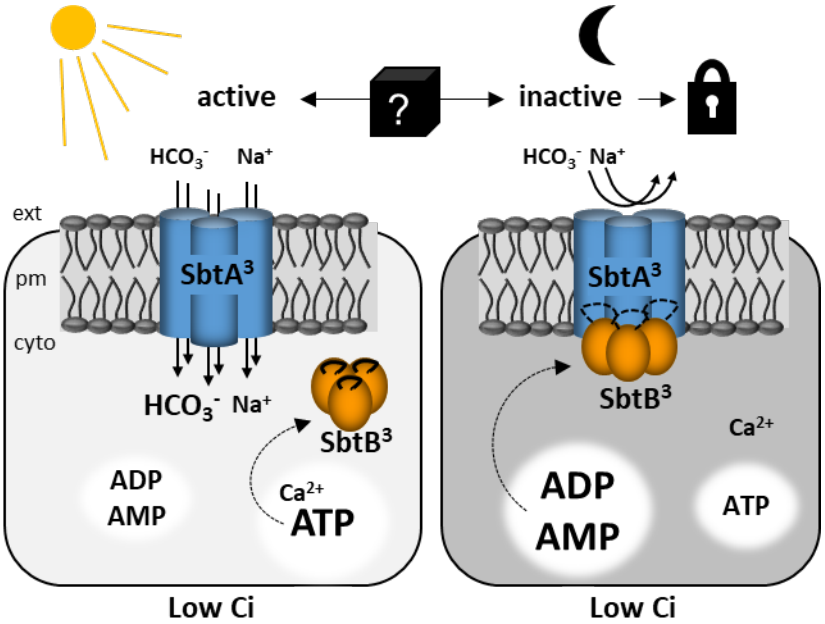

Fig. 8. Proposed regulation of SbtA bicarbonate transport activity by environmental stimuli and the adenylate energy charge (AEC). Expression of StbA and SbtB in *Synechococcus elongatus* is induced by low Ci availability in the light. Plasmamembrane (pm)-integral SbtA is actively transporting bicarbonate from the external environment (ext) into the cytoplasm (cyto) independent of SbtB, but depends on Na^+- symport and requires a cell-inward-directed Na^+ gradient. Functional SbtA is likely a homotrimer ($SbtA^3$) that transports HCO_3^- and Na^+ at a 1:1 stoichiometry through each monomer. Light-stimulated photosynthetic electron transport sustains high levels of intracellular ATP over ADP and AMP (high AEC), which facilitates binding of Ca^{2+}ATP to SbtB trimers ($SbtB^3$), stabilization of the SbtB T-loops, and SbtB remains dissociated from SbtA. However, causality between T-loop conformation and SbtA:SbtB interaction has not been proven yet. Upon transition from light to dark, a change from high to low AEC is likely to take minutes, yet SbtA-mediated bicarbonate uptake is inactive within 15 s. Potential, fast signals for SbtA dark-inactivation (and light-activation) remain speculative and may include changes in membrane potential, redox status, and/or post-translational modifications of SbtA and other regulatory proteins specific to photosynthetic cyanobacteria. In prolonged darkness, cells operate at a lower AEC. The relatively higher amounts of ADP and AMP replace ATP as ligands in SbtB trimers, which destabilizes the T-loops, and and stable SbtA:SbtB complexes of unknown stoichiometry are formed. Thus, SbtB may have a role as curfew protein, locking SbtA into its inactive state and preventing energetically wasteful and ineffective bicarbonate accumulation under photosynthetically unfavorable conditions.

Table 1. **Correlations between association of SbtA and SbtB proteins and adenylnucleotide ratios.**

Adenylnucleotides	SbtA	AR_{50}[a]	AR_{25}[a]	AR_{10}[a]
ATP:ADP	SbtA7001	0.55 ± 0.10	0.72 ± 0.06	0.86 ± 0.03
	SbtA7942	0.41 ± 0.14	0.57 ± 0.11	0.74 ± 0.08
ATP:AMP	SbtA7001	0.77 ± 0.03	0.85 ± 0.03	0.91 ± 0.04
	SbtA7942	0.53 ± 0.11	0.69 ± 0.09	0.85 ± 0.07
cAMP:ADP	SbtA7001	0.63 ± 0.11	0.81 ± 0.07	0.91 ± 0.04
	SbtA7942	0.62 ± 0.06	0.73 ± 0.05	0.83 ± 0.04
cAMP:AMP	SbtA7001	0.85 ± 0.08	0.91 ± 0.05	0.95 ± 0.03
	SbtA7942	0.58 ± 0.01	0.71 ± 0.01	0.83 ± 0.01

[a] Adenylnucleotide ratios corresponding to 50% (AR_{50}), 25% (AR_{25}) and 10% (AR_{10}) of SbtA bound to SbtB were estimated from sigmoidal logistic curve fits (Fig. S5). AR values (± SE) are averages of 3 to 4 independent experiments. AR values were statistically not significantly different at $P \leq 0.05$ between SbtA-SbtB pairs and for different adenylnucleotide combinations tested (AR_{50} $P = 0.232$, AR_{25} $P = 0.211$, AR_{10} $P = 0.275$).